SUMITOMO ELECTRIC TECHNICAL REVIEW
No. 98 · APRIL 2024
FEATURED TOPIC

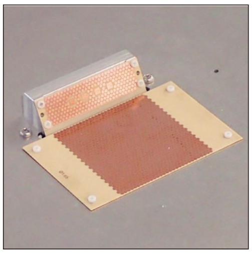

Automotive Antenna Using Metamaterial Technology Suitable for 5G mmWave Communication

Yutaro MIKI*, Suguru YAMAGISHI, Ichiro KUWAYAMA, and Kunio SAKAKIBARA

This paper reports on the development of an antenna suitable for 5G millimeter wave (mmWave) communication, incorporating metamaterial technologies such as Electromagnetic Band Gap (EBG) and Artificial Magnetic Conductor (AMC). The goal is to achieve automated driving by utilizing 5G, which offers high-speed, large-capacity, and low-latency features. To enable efficient data communication, particularly for sensing information, the use of mmWave band with a bandwidth of several hundred MHz is required. However, the use of an array antenna consisting of multiple patch antenna elements on the roof of a vehicle poses challenges in terms of radiation characteristics. This study aims to address these challenges through the development of an antenna suitable for 5G mmWave communication.

Keywords: 5G, automotive antenna, mmWave, metamaterial

1. Introduction

The government and private sectors are cooperating to promote various technology development projects for the implementation of automated driving. To enable proper cruise control during automated driving, it is necessary to acquire various data from other vehicles, roadside devices, servers, and the like, as well as to use the vehicle's own sensor data.(1) For communications for that purpose, candidate choices include using direct communication with other vehicles and mobile phone networks, where the communication system is required to be fast, large in capacity, and low in latency.

In Japan, fifth-generation mobile communications (5G) began to offer commercial services in March 2020(2) with three features—ultrafast/simultaneous multiple connections, low latency, and high reliability. The frequency bands used with 5G are divided into two frequency bands, which are a band under 6 GHz and a millimeter wave (mmWave) band (including those slightly longer than mmWaves). In Japan, in the 28 GHz band used as 5G mmWave, a frequency band as wide as 400 MHz is allotted to each telecommunications carrier.(3) This band is ideal for fast and large-capacity communications. Therefore, expectations are high for the use of 5G mmWave for the various above-mentioned data communications in automated driving.

AutoNetworks Technologies, Ltd. has worked on the development of automotive antenna technology suitable for 5G mmWave communications. This paper describes the challenges experienced when mounting a 5G mmWave antenna on an automobile and an antenna that applies metamaterial*1 technology as a solution to these challenges.

2. 5G mmWave Automotive Antennas

With 5G mmWave, antennas use beam-forming technology at both base stations and in user equipment. It is a technology that concentrates radio waves emitted by an antenna in a desired direction and enables radio waves to travel over long distances even in the mmWave band, in which the wavelength is short and the range attenuation is fast. Moreover, its concentration of emitted radio waves in a specific direction is effective in avoiding interference with other communications.

Beam forming uses an array antenna comprising multiple antenna elements. The direction in which radio waves are emitted can be changed by suitably controlling and combining the excitation amplitude and phase of each element of the array antenna.

Additionally, it is also necessary to support multiple-input and multiple-output (MIMO). The term MIMO refers to the use of multiple antenna systems for communications at both the transmitter and receiver ends. This technique improves the communication rate by increasing the data communication volume per unit time. With 5G mmWave, the polarized MIMO system is used in which the fields of the radio waves emitted from the antenna are oriented (polarized) such that the two polarized waves are orthogonal to each other.

Array antennas commonly used in the 28 GHz band allotted for 5G mmWave communications are patch antennas formed on a print circuit board (PCB) due to the ease of mass production and cost. The configuration of the patch array antenna discussed in this paper is shown in Fig. 1. The configuration is a four (horizontal)-by-one (vertical) arrangement for the purpose of horizontal beam forming. The patch antenna element is square-shaped. Each element has inputs for horizontally polarized (HP) and vertically polarized (VP) waves to support polarized MIMO.

Figure 2 presents a rendered image of a 5G mmWave antenna mounted on an automobile. MmWaves are characterized by the fact that obstacles greatly affect radio wave attenuation. Therefore, it is desirable that antennas are installed clear of obstacles in the surrounding area, so the antenna is assumed to be installed on the roof (Fig. 2 (a)). Normally, the communication partners, or base stations, are installed in an elevated location such as on the top of a building. Therefore, the rooftop array antenna is positioned facing obliquely upward. In this study, the antenna is angled at 60° with respect to the rooftop. By placing four-element array antennas—capable of beam forming between ±45° directions—in four directions in zones A to D at 90° intervals, it is possible to cover the full 360° horizontally (Fig. 2 (b)).

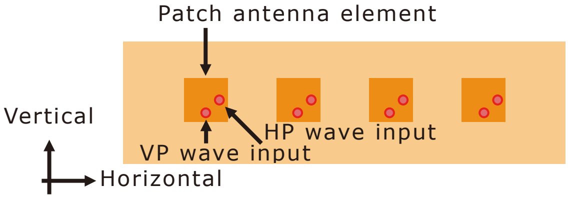

Fig. 1. Four-element patch array antenna model for study

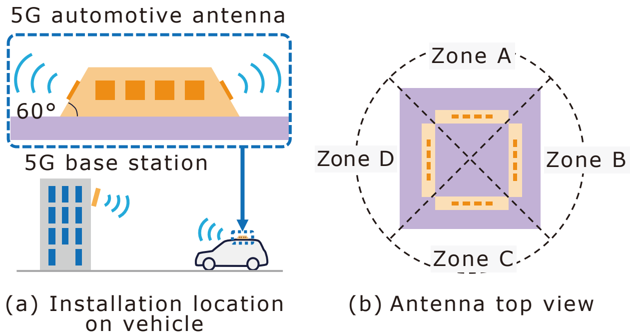

Fig. 2. Rendered image of array antenna installation and arrangement on an automobile

The installation of a 5G mmWave antenna on the roof of an automobile involves two challenges as described below. For each challenge, the mechanism underlying the occurrence of the challenge and a solution will be described.

3. Use of EBG for Mitigating Irregular Directivity Caused by Surface Wave Mode [Challenge 1]

While the frequency width per carrier allotted in Japan is 400 MHz, the overall bandwidth of 5G mmWave is 2,500 MHz from 27 GHz to 29.5 GHz. It is desirable that antenna design is common to all carriers, so it is necessary to ensure that the antenna operates throughout the 2,500 MHz bandwidth.

Figure 3 gives an example of configuration of the patch antenna elements. The structure features placement of the radiating elements and the ground (GND) on the opposite sides of a PCB, a dielectric material. The operating frequency band of a patch antenna is wider with increasing thickness of the dielectric material. The thickness of the dielectric material has been chosen to meet the requirements for operation within the bandwidth of 2,500 MHz. However, as a property of patch antennas, the surface wave mode increases with increasing thickness of the dielectric material. The surface wave mode is a component propagating on the GND surface, which, upon reaching an end of the GND, is radiated into the air, resulting in unwanted radiation. This unwanted radiation from the surface wave mode is combined with the forward component radiated from the radiating elements, acting as a factor causing irregular directivity of the antenna.

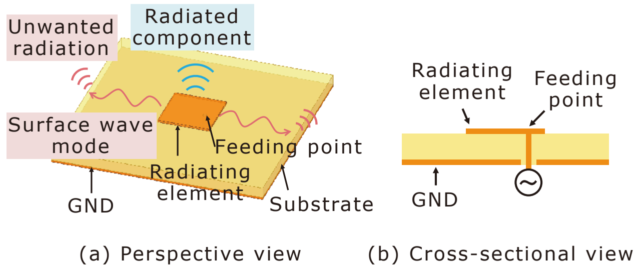

Fig. 3. An example of patch antenna configuration

The surface wave mode has the property of propagating strongly in the polarized direction of the radiating element. Accordingly, its impact on the directivity of HP and VP wave inputs is greater in the horizontal and vertical directions, respectively. In the currently studied configuration (Fig. 1), in which beam forming takes place in the horizontal direction, the irregular directivity in the horizontal plane of the HP wave is particularly problematic. We obtained simulation results for the studied model. Figure 4 (a) shows a distribution of the surface wave mode on an array antenna substrate observed when exciting the HP wave input of element 3 alone; Fig. 4 (b) illustrates the directivity observed when individually exciting each element. The surface wave propagates in the right and left directions in the illustration (Fig. 4 (a)), producing ripple-like dents and projections (irregularity) in directivity

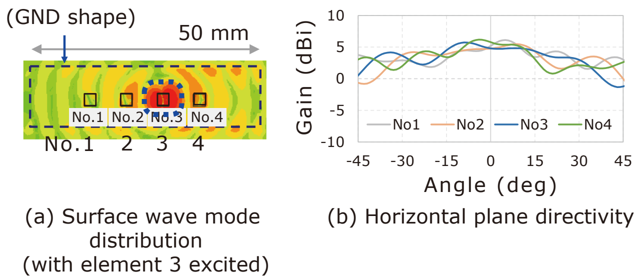

Fig. 4. Four-element patch array antenna simulation results of exciting HP wave input (28 GHz)

(Fig. 4 (b)). Because the directivity of an array antenna is the result of combining the directivity of each patch element, it is desirable to obtain a higher gain that the elements have uniform directivity. However, the elements differ from each other in directivity due to the effect of the surface wave mode, resulting in a failure to achieve the full benefits of increased gain through array combination.(4)

One of the techniques used to suppress the surface wave mode on the GND is to use an electromagnetic band gap structure (EBG). Figure 5 presents a schematic diagram of an EBG. Mushroom-shaped elements each consisting of a conductor patch and a metallic via periodically arrayed at fixed intervals are equivalent, as a circuit, to inserting capacitances in series and inductances in parallel. The result is a structure that has a band gap in which radio waves do not propagate.(5)

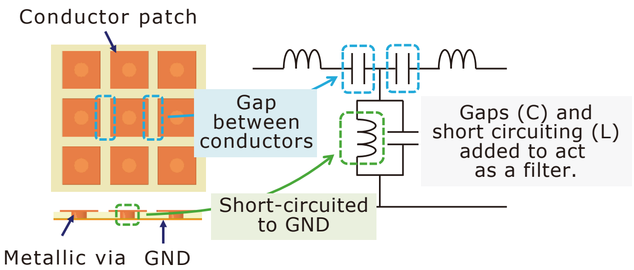

Fig. 5. Schematic diagram and equivalent circuit diagram of mushroom-shaped EBG

Figure 6 shows a structural diagram and the dimensions of the mushroom-shaped EBG employed in this study. The conductor patches are regular hexagonal so as to be densely placed around the radiating elements of the patch antenna. When being designed, the patch element size, gaps between elements, via diameter and other parameters were appropriately selected.

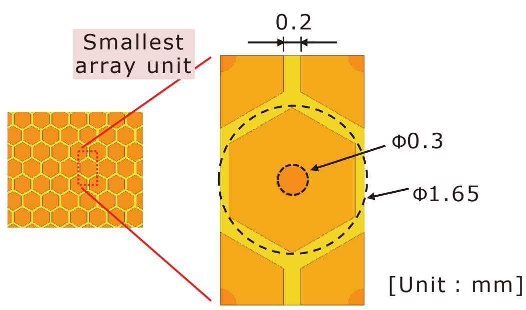

Fig. 6. Regular hexagonal mushroom-shaped EBG

The simulation results of the designed EBG are given in Fig. 7 as a dispersion diagram representing band gap characteristics. The band gap is the frequency range in which no eigenfrequencies exist between Mode 1 and Mode 2. The simulation results show that the band gap is

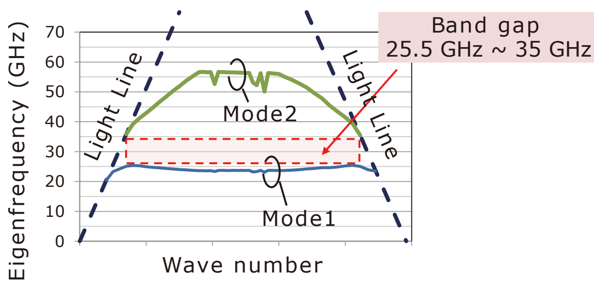

Fig. 7. Band gap characteristics of designed EBG (dispersion diagram)

from 25.5 GHz to 35 GHz, which contains the 5G mmWave frequency band of 27 GHz to 29.5 GHz.

This EBG loaded on the four-element patch array antenna was simulated. Figure 8 (a) shows a distribution of the surface wave mode on an array antenna substrate when exciting the HP wave input of element 3 alone; Fig. 8 (b) illustrates the directivity observed when individually exciting each element. The surface wave mode is suppressed as anticipated, and each element exhibits uniform directivity.

As with the simulation, the prototype evaluation results—described in Chapter 5 (Fig. 15 (a))—revealed the occurrence of irregular directivity attributable to the surface wave mode and the suppression of irregular directivity owing to the loading of the EBG.

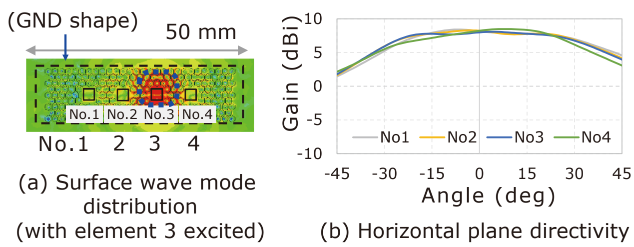

Fig. 8. Four-element patch array antenna simulation results of exciting HP wave input with EBG loaded (28 GHz)

This paragraph describes the effect of the improved directivity of a discrete patch antenna element on the increased combined gain of the array antenna.(6) Using the simulation results presented in Figs. 4 and 8, calculations were conducted to determine the combined directivity of the array antenna during beam forming. The excitation phases of elements 1 to 4 were adjusted and the peak angle of combined directivity was shifted at 20° intervals between –40° and +40°. The resultant horizontal directivity is illustrated in Fig. 9. Notably, the gain of (a) antenna with the EBG is approximately 3 dB higher than that of (b) antenna without the EBG, at a peak angle of 0°. In addition, it was verified that the loading of the EBG is effective in improving the gain under all peak angle conditions.

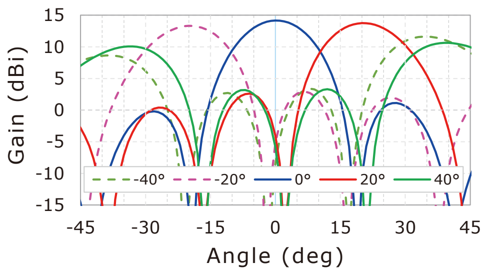

(a) With EBG

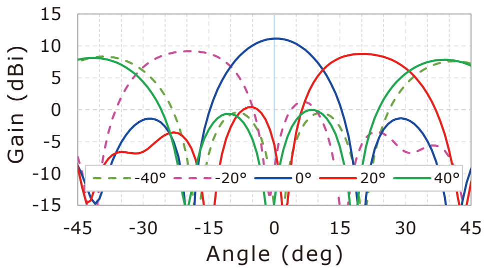

(b) Without EBG

Fig. 9. Combined horizontal plane directivity of four-element array antenna (HP wave input, 28 GHz)

4. Use of AMC to Prevent Nulls Caused by Reflections from Roof [Challenge 2]

The installation of an antenna on a vehicle roof involves another challenge, which is the occurrence of nulls (little or no radio power) in the vertical plane directivity of vertically polarized waves.(7)

We conducted a simulation of a single element of the patch antenna placed at an angle of 60° with respect to the roof, which is a conductive plate, as illustrated in Fig. 2 (a) in Chapter 2. The simulation model is presented in Fig. 10 (a). The directivity of the VP wave input in the vertical plane (zx plane in the illustration) is shown in Fig. 10 (b). The challenge is the occurrence of a sharp null near 67°, which makes communications impossible when the base station is in the null direction.

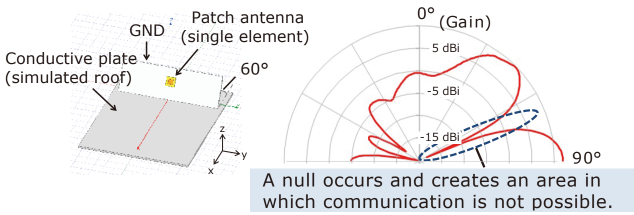

(a) Model diagram (b) Vertical plane (zx plane) directivity

Fig. 10. Vertical directivity of a patch antenna installed on a conductive plate (VP wave input, 28 GHz)

Figure 11 illustrates the underlying principle behind the occurrence of a null in vertical plane directivity under this condition. The vertical plane directivity results from the combination of the direct waves from the patch antenna's radiating element and the reflected waves from the roof, a conductor. In an instance where these waves have similar amplitudes and opposite phases, the radio waves are canceled, producing a null in the vertical plane directivity.

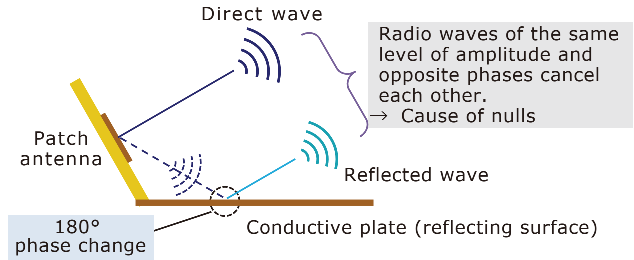

Fig. 11. Principle behind the occurrence of directivity nulls

As a solution to the null, a structure was employed to place an artificial magnetic conductor on the reflecting surface. When reflected on a conductive plate, the phase of radio waves changes by 180° with respect to the incident radio waves. By loading an AMC on the reflecting surface, however, it becomes possible to change the phase of the reflected waves. Noting this feature of the AMC, we attempted to prevent nulls.

The AMC is structured to have periodically arrayed mushroom-shaped elements as with the EBG. Figure 12 presents the results of simulating reflected phase versus incident angle as the characteristics of an AMC provided with the same dimensions as the EBG design conditions described in Fig. 6 in Chapter 3. In contrast to waves reflected by a conductor plate undergoing a 180° phase change at any incident angle, loading of an AMC causes waves to undergo a phase change between 0° and +90°.

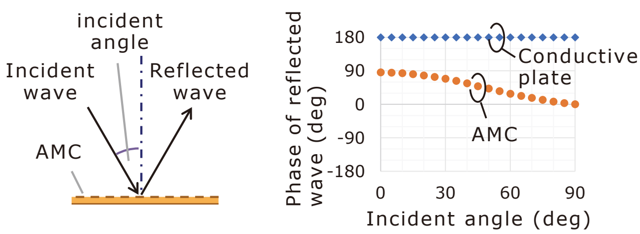

Fig. 12. Phase of reflected waves versus incident angle of the designed AMC (28 GHz)

This AMC was simulated being placed on a conductive plate representing a roof. Figure 13 plots the vertical plane directivity observed after loading of the AMC. A comparison between before and after loading the AMC reveals that the null occurring at around 67° disappeared, enabling communications in this angular direction. Additionally, Fig. 14 shows the results of the comparison, determined through simulation, of field strength distribution in the vertical direction with and without the AMC. A null area exists (a) when the AMC is absent, resulting from interference between the direct waves from the patch antenna and the reflected waves from the conductive plate, while the null is eliminated (b) when the AMC is loaded because the AMC changes the phase of the reflected waves and avoids interference, enabling communications in this angle range.

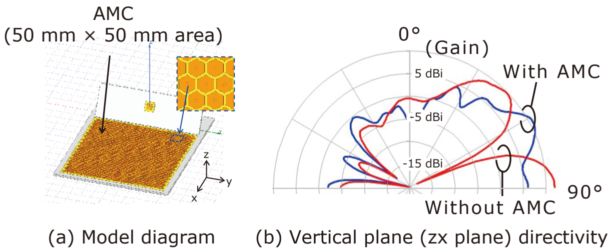

Fig. 13. Vertical plane directivity of a patch antenna installed on a conductive plate with AMC loaded (VP wave input, 28 GHz)

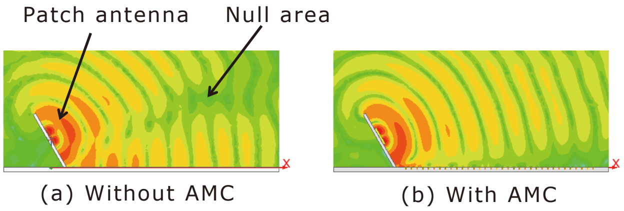

Fig. 14. Field strength distribution with and without AMC (VP wave input, 28 GHz)

5. Prototype Antenna Evaluation Results

A prototype antenna was constructed based on the simulation results, with an EBG loaded around the patch array antenna and with an AMC loaded on a conductor plate simulating a roof. Photos 1 and 2 show the prototype antenna and the directivity measurement setup, respectively. In addition, Fig. 15 gives the results of directivity measurement after only exciting element 3 of four elements. A prototype antenna without the EBG and AMC was also constructed and measured for comparison purposes.

Regarding horizontal plane directivity (Fig. 15 (a)) and vertical plane directivity (Fig. 15 (b)), the prototypes were observed to mitigate irregular directivity in the horizontal plane described in Chapter 3 and to prevent the occurrence of nulls described in Chapter 4. Thus, the effects of the EBG and AMC-loaded antenna were also demonstrated by prototypes.

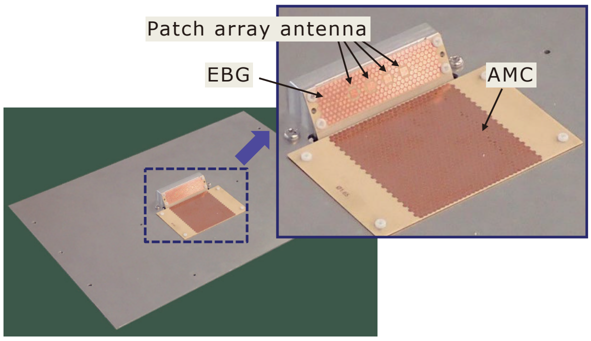

Photo 1. EBG and AMC-loaded prototype antenna

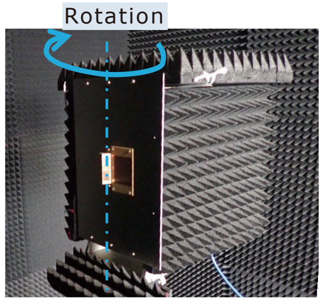

Photo 2. Directivity measurement setup for prototype antennas (vertical plane)

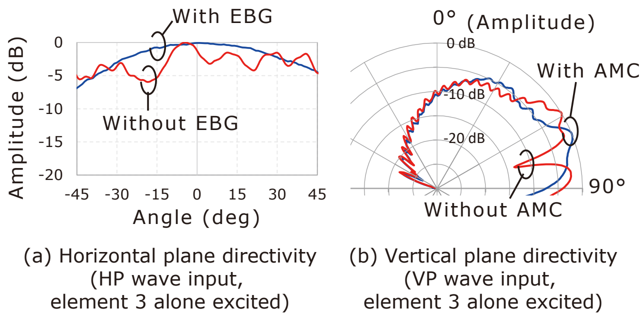

Fig. 15. Prototype antenna directivity measurement results (28 GHz)

6. Conclusion

This paper described two challenges involved in the mounting of a 5G mmWave-communication array antenna on an automobile roof, along with an explanation of the occurrence mechanisms and solutions to the challenges achieved by applying metamaterial technology. An antenna with performance tailored to automotive conditions was developed, which, through the application of EBG and AMC techniques, solved irregular directivity in the horizontal plane caused by the surface wave mode and the occurrence of nulls in vertical plane directivity due to reflection by the roof. We hope that this technology will be utilized to help accelerate the creation of an automated driving society.

Technical Term

∗1 Metamaterial: An artificial functional material designed to exhibit functionalities that are not naturally present (such as : negative permittivity) by arranging structures smaller than the wavelength periodically.

References

(1) K. Sakaguchi, et al., "Towards mmWave V2X in 5G and Beyond to Support Automated Driving," IEICE Transactions on Communication, vol. E104–B, no.6 (June 2021)

(2) The Fifth Generation Mobile Communications Promotion Forum (5GMF) Millimeter Wave Promotion Ad Hoc, "Summary of 5GMF White Paper Ver.2.0" (September 2023)

(3) Ministry of Internal Affairs and Communications, JAPAN, "Establishment Plans for Specified Base Stations for Diffusion of 5G Mobile Communications Systems" (April 2019)

(4) S. Yamagishi, "Studies on mmWave Antenna Using Print Circuit Board," IEICE Technical Report, AP2022-20 (June 2022)

(5) D. Sievenpiper, L Zhang, R. F. Jimenez Broas, N. G.Alexopolous, and E. Yablonovitch, "High-Impedance Electromagnetics Surface with a Forbidden Frequency Band, " IEEE Transactions on Microwave Theory and Techniques, Vol. 47, No. 11, pp.2059 –2074 (November 1999)

(6) Y. Miki, S. Yamagishi, I. Kuwayama, K. Sakakibara, "Improvement in Directivity of Patch Array Antenna with EBG," 2021 IEICE General Conference, BS-1-1 (March 2021)

(7) Y. Miki, S. Yamagishi, I. Kuwayama, K. Sakakibara, "Improvement in Vertical Radiation Pattern of mmWave Band Antenna with AMC," 2022 IEICE General Conference, B-1-133 (March 2022)

Contributors

The lead author is indicated by an asterisk (∗).

Y. MIKI∗
• Group Manager, AutoNetworks Technologies, Ltd.

S. YAMAGISHI
• General Manager, AutoNetworks Technologies, Ltd.

I. KUWAYAMA
• Senior Assistant General Manager, AutoNetworks Technologies, Ltd.

K. SAKAKIBARA
• Doctor of Engineering
Professor, Nagoya Institute of Technology